




Flexible behaviour in a mesopelagic fish (*Maurolicus muelleri*)

Svenja Christiansen ^{1,*}, Thor A. Klevjer², Anders Røstad ³, Dag L. Aksnes⁴, and Stein Kaartvedt ¹

¹Department of Biosciences, University of Oslo, Blindern 0316, Norway

²Institute of Marine Research, Bergen 5817, Norway

³Red Sea Research Center, King Abdullah University of Science and Technology, Thuwal 23955-6900, Saudi Arabia

⁴Department of Biological Sciences, University of Bergen, Bergen, Norway

*Corresponding author: tel: +47 228 54242; e-mail: svenja.christiansen@ibv.uio.no.

Christiansen, S., Klevjer, T. A., Røstad, A., Aksnes, D. L., and Kaartvedt, S. Flexible behaviour in a mesopelagic fish (*Maurolicus muelleri*). – ICES Journal of Marine Science, doi:10.1093/icesjms/fsab075.

Received 9 October 2020; revised 24 March 2021; accepted 26 March 2021.

Variability of mesopelagic scattering layers is often attributed to environmental conditions or multi-species layer composition. Yet, little is known about variation in behaviour among the individuals forming scattering layers. Based on a 10 months high-resolution dataset from stationary echosounders in a Norwegian fjord, we here assess short-term and long-term behaviour of a single mesopelagic fish species, the pearlside *Maurolicus muelleri*. The daytime vertical extension of the monospecific pearlside scattering layers spanned four orders of magnitude ambient light in the autumn and winter and less than one order of magnitude in summer. While the main layers tracked relatively stable light levels over daytime, some individuals actively crossed light gradients of up to 1.5 orders of magnitude. This included individuals that moved between scattering layers, and apparently bold individuals that made regular upward excursions beyond the main population distribution. During the daytime, *M. muelleri* mitigated the risk of predation by forming tight groups in the upper scattering layer and, at light levels $>10^{-6} \mu\text{mol m}^{-2} \text{s}^{-1}$, by instantly diving into deeper waters upon encounters with predators. Our observations suggest that individual, and probably state-dependent, decisions may extend the pearlsides' vertical distribution, with implications for predator–prey interactions.

Keywords: individual behaviour, light, predator avoidance, scattering layer variability, social aggregation, stationary echosounder

Introduction

The enormous mesopelagic, or twilight, zone lies below the sunlit euphotic ocean but still receives enough light to allow for visual predation by adapted animals. The complexity of mesopelagic vertical distribution became evident already soon after the discovery of deep scattering layers (Duvall and Christensen, 1946; Eyring *et al.*, 1948): often, multiple sound scattering layers are present, and net catches at mesopelagic depths revealed a high number of species present (Barham, 1957; 1966; Pearcy *et al.*, 1977). The most apparent behavioural pattern of deep scattering layers is their diel vertical migration (Welsh *et al.*, 1937) in tight synchrony with ambient light (Duvall and Christensen, 1946; Kampa and Boden, 1954; Dickson, 1972), although parts of layers may not migrate (Dietz, 1948). Contemporary mesopelagic

research focuses on quantifying biomass (Davison *et al.*, 2015; Proud *et al.*, 2019), harvest potential (Prellezo, 2019; Grimaldo *et al.*, 2020), food webs, and active vertical carbon transport (Hudson *et al.*, 2014; Belcher *et al.*, 2019), and would benefit from increased knowledge on the vertical behaviour of the animals of the scattering layers.

Animal behaviour and distribution are influenced by external and internal factors. Usually, the variability in the vertical distribution of scattering layers is correlated with environmental variability (Béhagle *et al.*, 2016; Urmy and Horne, 2016; Proud *et al.*, 2017; Boswell *et al.*, 2020) or attributed to differences in species composition (Gauthier *et al.*, 2014; Benoit-Bird *et al.*, 2017). Less knowledge exists about the variability in behaviour within species; High species diversity, often more than a hundred species

© International Council for the Exploration of the Sea 2021.

This is an Open Access article distributed under the terms of the Creative Commons Attribution License (<http://creativecommons.org/licenses/by/4.0/>), which permits unrestricted reuse, distribution, and reproduction in any medium, provided the original work is properly cited.

(Ariza *et al.*, 2016; Wang *et al.*, 2019), within oceanic scattering layers may prohibit unravelling such species-specific variability.

In contrast, scattering layers in Norwegian fjords resemble their oceanic counterparts in their dynamics but contain only a few species (Giske *et al.*, 1990). Fjord ecosystems therefore provide an opportunity to observe how variations in scattering layers are affected by individual behaviour within species. The pearlside *Maurolicus muelleri* forms nearly monospecific scattering layers in Norwegian fjords (Giske *et al.*, 1990; Staby *et al.*, 2011). Fish of the genus *Maurolicus* have a world-wide distribution (Rees *et al.*, 2020) and are known for their relatively high abundance in the upper mesopelagic (Gauthier *et al.*, 2014; Escobar-Flores, 2019). Pearlsides have a distinct vertical migration behaviour which is strongly influenced by season (Prihartato *et al.*, 2015; Staby *et al.*, 2011) and ontogeny (Giske *et al.*, 1990; Baliño and Aksnes, 1993; Staby *et al.*, 2013), and characterized by immediate reactions to changes in ambient light (Baliño and Aksnes, 1993; Staby and Aksnes, 2011), s.a. Supplementary Figure S1. This light-associated behaviour has been interpreted as a way to optimize vision-based food intake over vision-based predation risk (Clark and Levy, 1988; Giske *et al.*, 1990). As a result, the fish are expected to occupy a certain window of light intensities that has been referred to as “antipredation window” (Clark and Levy, 1988) and “light comfort zone” (Røstad *et al.*, 2016). Since individuals within a population will probably vary in hunger and energy reserves we hypothesize that deviating, “atypical” behaviour for some of the individuals exists.

Deviations from the average and thus individual variation ultimately drive evolution (Allen and McGlade, 1987). Processes with atypical outcomes may have large ecological consequences: For example, in studies of a reef fish population, Allgeier *et al.* (2020) showed that subsets of the population have a disproportional impact on nutrient production. Furthermore, “unusual” daytime schooling in the epipelagic by the mesopelagic fish *Vinciguerria nimbaria* contributes to sustaining tuna populations in the Atlantic Ocean (Marchal, 1996).

We analysed a 10-month long dataset of moored echosounders complemented with net sampling at the start and end of the registration period, for a fjord population of *Maurolicus*. The acoustic records provided continuous and high-resolution data throughout the water column, allowing for quantifying variability at various temporal and vertical scales for both populations and individuals. We relate these observations to light conditions, discuss possible implications, and suggest hypotheses to be tested in future studies of mesopelagic scattering layers.

Material and methods

Study site (Masfjorden)

Masfjorden is a sheltered fjord on the West coast of Norway. It is about 20 km long, 0.5–1.5 km wide and has a maximum depth of 494 m. The fjord is connected to the more open Fensfjorden via a sill at 75 m depth. Due to this sill, water masses are generally homogenous below ~80 m depth, with salinities > 34.9 and temperatures of ~8°C (Aksnes *et al.*, 2019). During the current study (2010/11), dissolved oxygen concentrations were >3 ml l⁻¹ throughout the water column (Aksnes *et al.*, 2019).

Trawl catches

We used a pelagic trawl (100 m² net opening; square mesh size 20 cm × 20 cm declining to 3 mm × 3 mm in the cod-end), for assessing the mesopelagic community composition at the

beginning (8–11 October 2010) and end (14–18 August 2011) of the study period. The trawl was equipped with a Multisampler, holding three independent cod ends that could be opened and closed on command from the vessel (Engås *et al.*, 1997). We made 19 successful deployments in 2010 and 9 in 2011. Due to logistic constraints including very short summer nights in August, nocturnal sampling was limited. Each deployment was restricted to one depth layer, thus providing three consecutive “replicates”, with the individual cod ends in most cases being opened for 10 min at ~2 knots tow speed. We allowed between 1 and 5 min for flushing of the trawl between closing the previous and opening the next cod end, thereby reducing contamination between nets. In total, 70 trawl samples were sorted, weighed, and counted upon retrieval. We here normalize the catch by dividing total numbers by the number of minutes trawled. Average individual weight was obtained by dividing the total number of individuals by the total weight, for each species.

Acoustic measurements

We deployed three upward-looking SIMRAD EK60 split-beam echo sounders (7.1° beam angle) in Masfjorden (~60° 50'N, ~5° 30'E), from 7 October 2010 to 15 August 2011 (s.a. Prihartato *et al.*, 2015). The submerged transceivers were kept in pressure-proof casings and cabled to a shore station for power supply and data storage. The echo sounders were mounted at the bottom (38 kHz; ~370 m; 512 μs; 1 ping s⁻¹) and in rigs floating at ~280 m (120 kHz; 256 μs; 1–2 pings s⁻¹) and ~90 m (200 kHz; 128 μs; 1–2 pings s⁻¹) in close vicinity to each other. The echo sounders were calibrated at the surface using standard methods (Foote *et al.*, 1987). We here mostly use data at 120 kHz, supplementing with records from the two other frequencies. We show representative echograms displaying mean volume backscattering strength (S_v; dB re 1 m⁻¹; MacLennan *et al.*, 2002) at selected days of the study period to exemplify different behaviours.

Scattering layer properties

We determined the vertical location and range, as well as backscatter properties of the noon (±15 min) *Maurolicus* scattering layers for each day of the study period. We prepared the 120 kHz S_v data by binning (averaging in the linear domain) into 0.5 m and 1.44 min intervals. Then, we excluded parts of the echogram where the binned S_v values were larger than the 95th percentile of the S_v data to reduce the influence of strong echoes by larger fish (Supplementary Figure S2). For the remaining data, we calculated the backscatter anomaly by subtracting the running median (window size 5 datapoints, i.e. ~7.2 min) of the S_v values in each depth bin. The backscatter anomaly represents the ratio of *Maurolicus* backscatter to background values (averaged over time) for each depth bin. Then, we defined the 5th, 25th, 75th, and 95th percentile of the backscatter anomaly such that we obtained depth profiles of backscatter anomaly percentiles. To be classified as a layer, more than 75% of the bins in one depth had to be stronger than the median over at least five consecutive depths (2.5 m). An additional condition was that the median of the S_v at those depths was > -70 dB to exclude plankton layers. The detected layers were numbered and their minimum, maximum, and depth range, as well as their mean S_v (calculated in the linear domain) determined.

We determined the upper edge of the shallowest scattering layer for selected days of the study period (dates where light

extinction was measured ± 3 days). For this purpose, the respective binned daytime data were smoothed (running median with window size 10 datapoints, i.e. 14.4 min and 5 m). Then, the upper edge of the daytime layer was defined as the shallowest point in the echogram which exceeded an empirically determined S_v threshold of -70 dB (January) or -65 dB (all other months) over at least 5 m depth, for each timepoint between sunrise and sunset.

Boldness

On some days, individuals of *Maurolicus* were located shallower than the main scattering layers. To get an impression of the extent of such apparently bold behaviour by individuals ascending into more illuminated waters, we quantified when and where such behaviour appeared by comparing it to the main population. We did this in conjunction with the layer detection (see previous section). To be detected as bold individuals the 5th percentile of the backscatter anomaly had to be >0 . In addition, the respective depth bins also had to be defined as a non-layer and the 75th percentile of S_v had to be >-70 dB. The conditions for the layer and bold individual detection were tested empirically for several days within the study period. Adjoining depth bins labelled as bold individuals were combined as vertical sections, numbered, and their properties determined (same as for the layers). For an individual section to be defined as bold individuals, that section had to be shallower than the shallowest scattering layer. Only the bold individuals closest to the shallow layer were selected.

Velocity

We determined vertical swimming velocities of selected individuals using the acoustic post-processing program Sonar5-Pro (Balk, 2019). Individual fish could be identified by their echo traces and in some cases followed over several minutes. We marked and saved the range and time of the beginning and end of such echo traces with the mouse-tip logger. By dividing the range difference by the time difference, we obtained the vertical speed of that individual between the two points. Note that the speeds obtained by this method do not include information on horizontal swimming.

Potential predators and escape reactions

Maurolicus muelleri is preyed upon by gadoid fishes (Giske *et al.*, 1990) which can be identified as strong echo traces on the echograms. We often observed that pearlsides near such strong echo traces of potential predators dived suddenly. To get an overview of the times, depths, and light levels at which “dive reactions” occurred, we visually scanned the 120 kHz echograms from 21 days, evenly distributed between 15th December 2010 and 15th August 2011, in intervals of 30 min and 25 m depth, respectively. Each occurrence of a strong echo trace (usually > -45 dB) was classified depending on the apparent interaction with the pearlsides as (i) pearlsides absent, (ii) present but no reaction, or (iii) dive reaction. The respective time and depth were saved and used for obtaining estimates of light levels for each occurrence.

Light

Surface photosynthetically active radiation (PAR, 400–700 nm) was measured continuously with a calibrated LI-190 quantum sensor (lower sensitivity threshold of $1 \times 10^{-4} \mu\text{mol m}^{-2} \text{s}^{-1}$) from 10th December 2010 to the end of the study period

(see Prihartato *et al.*, 2015 for details). On five days in 2011 (26th January, 22nd February, 11th April, 16th June, and 16th August), water column PAR (400–700 nm, with a resolution of 3.3 nm) was measured around noon with a RAMSES ACC hyper-spectral radiometer (Trios-optical sensors, Oldenburg, Germany). Measurements were made at depths around 1, 5, and 10 m and then every 10 m down to around 90–95 m depth (Prihartato *et al.*, 2015). In August, three replicate measurements were recorded for every metre (<15 m depth) and then for every 5 m. In June, the 40 and 50 m measurements were unreliable and therefore treated as missing values. Simultaneous surface measurements enabled the calculation of light attenuation coefficients (K ; m^{-1} ; integrated for the full spectrum measured in the profiles, s.a.; Table 1), which we used to estimate PAR in the water column similar to Prihartato *et al.* (2015). Below the deepest available measurements, we assumed a constant attenuation coefficient of 0.0739 m^{-1} (K_d ; m^{-1}) that was obtained by averaging all measured K_s from depths > 50 m. Thus, starting with the 90 m relative PAR estimate (i.e. given as a fraction of the surface light) obtained from the method used in Prihartato *et al.* (2015), we calculated the relative PAR at consecutive depths by extrapolation, using

$$E_z = E_{z-1} * \exp(-K_d) * \Delta z. \quad (1)$$

E_z is the relative PAR at depth z , E_{z-1} is the relative PAR at the previous (shallower) depth, K_d is the attenuation coefficient for depths > 90 m and Δz is the depth difference between the previous and current depth. The absolute ambient PAR was obtained by multiplying the surface PAR measurement with the relative PAR at the respective time and depth. Note that the extrapolated PAR values are very dependent on K_d and are prone to uncertainties since K_d might not be constant below 90 m. We estimated the light span (orders of magnitude) inhabited by *M. muelleri* from K_d and the respective depth range using:

$$\text{lightspan} = -\log_{10}(\exp(-K_d * \text{depth range})). \quad (2)$$

Results

Community composition

The main taxa in the trawl catches were *Maurolicus muelleri*, *Benthosema glaciale*, krill (*Meganyctiphanes norvegica* and *Thysanoessa* sp.), and pelagic shrimps (*Pasiphaea* and *Sergestes*). *Maurolicus muelleri* was the prevailing fish captured in the daytime scattering layers of the upper 100–200 m and the only fish caught in the shallowest layer (<70 m) in October 2010 (Figure 1). At about 200 m, there then was a mixture of *M. muelleri* and *B. glaciale*. In August, the shallowest layer was located at ~ 200 m, and *M. muelleri* was the only abundant target, with catches of 10000–30000 individuals in the three replicates. In slightly deeper tows, just beneath the core of this layer, numbers decreased. *Maurolicus muelleri* was still prevailing, but also *B. glaciale* were caught in these tows. *Benthosema glaciale* by far became the prevailing fish in the deeper tows, where also pelagic shrimps were common. Nocturnal sampling was limited to October. *Benthosema glaciale* and *Sergestes* then made up a considerable proportion ($\sim 20\%$) of the catches by number at 70 m depth during the early night (Figure 1c; trawl number 14–16).

Mysids (*Boreomysis arctica*) were numerous at depth, but are not included because of their small size (ca. 2 cm) and expected

Table 1. Light attenuation coefficients (K ; m^{-1}) between consecutive depths in Masfjorden in 2011.

Depth (m)	26 January 2011	22 February 2011	11 April 2011	16 June 2011	16 August 2011
0.5–5	0.283	0.176	0.299	0.491	0.275
5–10	0.116	0.174	0.143	0.272	0.195
10–20	0.096	0.131	0.177	0.203	0.141
20–30	0.081	0.109	0.079	0.209	0.122
30–40	0.076	0.089	0.141	NA	0.100
40–50	0.076	0.07	0.118	NA	0.086
50–60	0.079	0.059	0.067	0.088	0.078
60–70	0.083	0.06	0.068	0.085	0.072
70–80	0.072	0.034	0.078	0.061	NA
80–90	0.078	0.044	0.058	0.094	NA
>90			0.0739		

Below 90 m depth, we assumed a constant K that is the average of all K s measured at depths > 50 m.

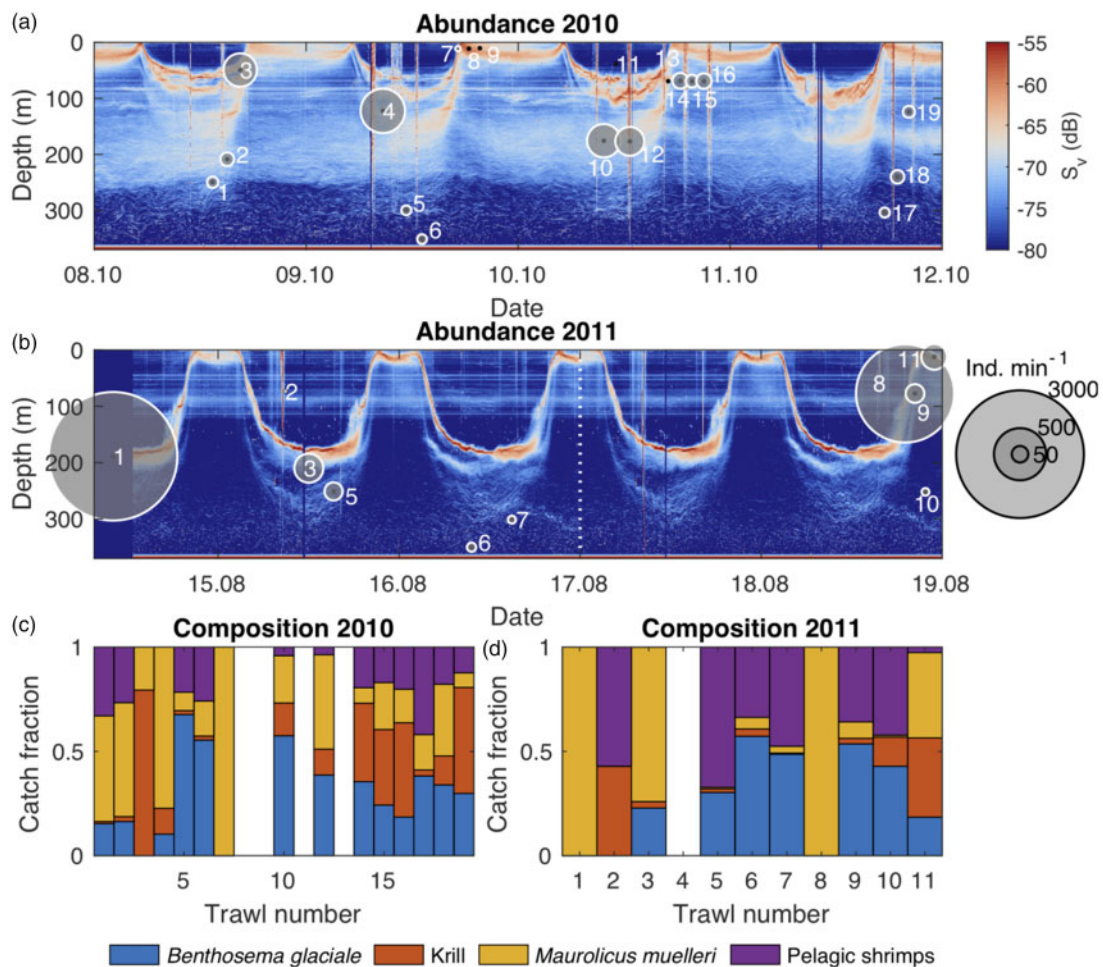


Figure 1. Location of trawl samples in October 2010 (a) and August 2011 (b), overlaid over the in-parallel obtained echogram from the submerged 38 kHz echosounder. Bubble sizes indicate the total number of individuals caught, normalized to sampling effort. As the 38 kHz echosounder was retrieved on the 17th August, the data from the two previous days are repeated on the 17th and 18th August (right of the vertical, dotted line). Panels (c) and (d) show the relative composition of the trawl catches with the numbers on the x-axis corresponding to the numbers in (a) and (b), respectively. Note that few krill were caught on the 14th August (trawl number 1 in 2011), but not quantified. Empty bars represent trawl catches that were not quantified.

negligible backscatter (Rudstam *et al.*, 2008). Gelatinous zooplankton including the siphonophore *Lensia* sp. (not pneumatophore-bearing and thus not strongly scattering), and scyphozoan jellyfish were regularly caught, but in small numbers, and are

therefore not included in the graphs. The in general small contributions to the acoustic backscatter from the invertebrates are substantiated by the data at 38 kHz (Figure 1), which basically mirror those at 120 kHz (e.g. Figure 2).

Maurolicus muelleri had average individual weights between about 0.2 and 1.25 g while *B. glaciale*'s weights ranged between 0.25 and 3.4 g (Supplementary Figure S3). Both species had a larger average weight at greater depths, with *B. glaciale* getting three times as heavy (about 2.5–3 g fish⁻¹) as *M. muelleri* (about 0.8 g fish⁻¹).

Population behaviour

The vertical extension of the pearlside distribution varied by a factor of ~ 6 throughout the sampling period, spanning 4 orders of magnitude ambient light in the autumn and <1 order of magnitude in summer (Table 2, Figures 2 and 3). Changes of the population distribution patterns happened over different time scales, from days (fusion of layers in April) to months (e.g. proportion of migrating adults in winter). In autumn, the *M. muelleri* population (defined as the scattering layers in the upper ~ 200 m based on the trawl catches) separated into two main scattering layers, ranging over ~ 120 m of the water column (Figure 1). The shallower layer performed diel vertical migration and usually separated into several sublayers in the upper 150 m during the day. The deeper main layer largely remained at mesopelagic depth

>150 m throughout the diel cycle (Figure 1). Between January and April, an increasing proportion of the deeper layer resumed diel vertical migration (e.g. Figure 2). After the fusion of the shallow and deep part of the population in mid-April, the vertical range of the population got narrower (Figures 2 and 3). Around midsummer usually only one, very narrow (less than 20 m), scattering layer existed (Figures 2 and 3, Supplementary Figure S4).

The daytime light exposure of the scattering layers changed over the season. During winter, the upper edge of the shallow layer moved along with the $\sim 10^{-2} \mu\text{mol m}^{-2} \text{s}^{-1}$ isolume (e.g. Figure 2, Table 2). The deeper layer during that season followed approximately the $\sim 10^{-4} \mu\text{mol m}^{-2} \text{s}^{-1}$ isolume (Table 2). In spring and summer, the deeper layer moved into darker conditions, until the upper part of the layer followed the $\sim 5 \times 10^{-5} \mu\text{mol m}^{-2} \text{s}^{-1}$ isolume in August. In the afternoon, the upper edge of the shallowest scattering layer crossed the $10^{-4} \mu\text{mol m}^{-2} \text{s}^{-1}$ and sometimes even the $10^{-2} \mu\text{mol m}^{-2} \text{s}^{-1}$ isolume (Figure 2). This result may in part be an artefact due to our assumption that light attenuation is independent of time of day (i.e. independent of the angular distribution of incoming sunlight). Therefore, we mainly restrict our discussion to the light conditions outside the migration periods.

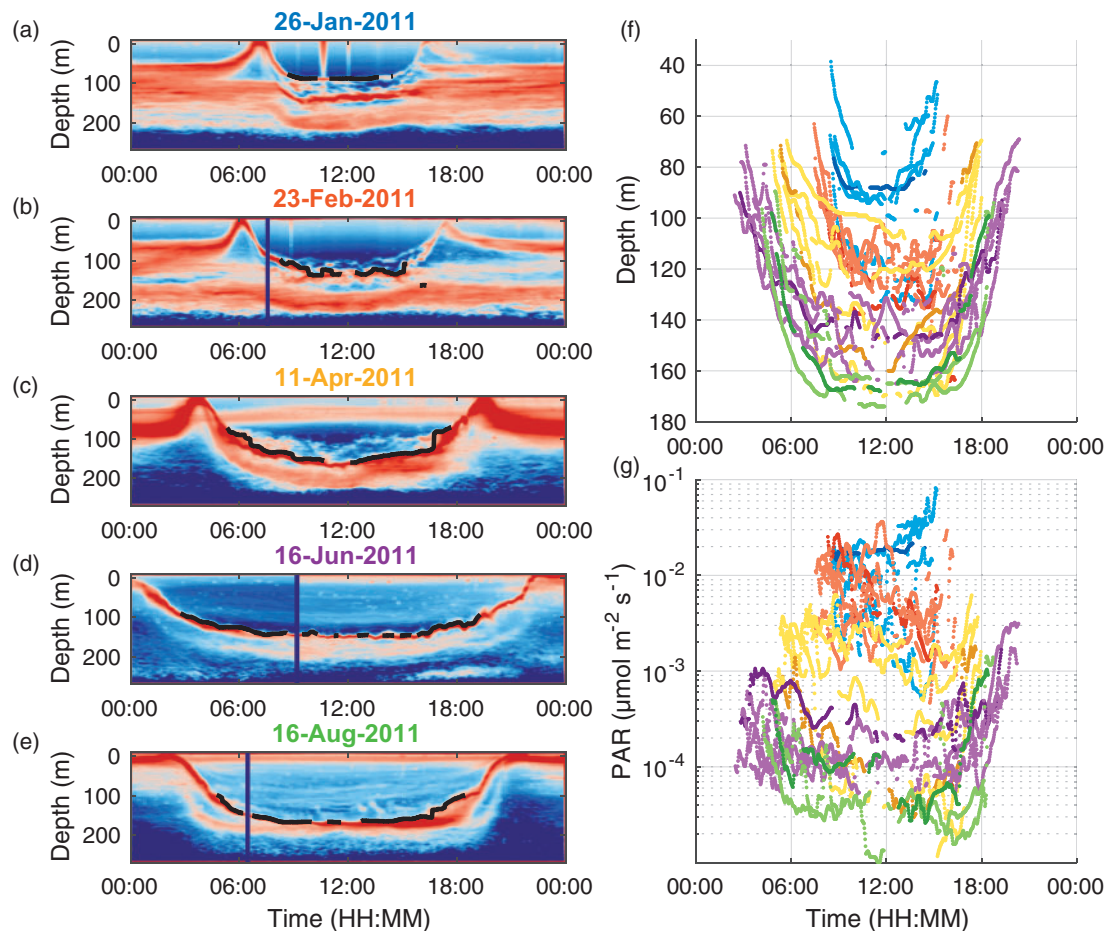


Figure 2. Echograms from the 120 kHz echosounder on the five dates where light attenuation was measured (a–e). The black lines indicate the upper edge of the shallowest scattering layer. Depth (f) and light (PAR) (g) at the upper edge of the shallowest scattering layer on the same dates (colours as in the titles in the left). In addition, we have included three days just before and after the measurement day (lighter colours).

Table 2. Scattering layer properties around noon on the days where light attenuation was measured.

	Layer	26 January 2011	22 February 2011	11 April 2011	16 June 2011	16 August 2011
Min depth (m)	Shallow	99	134	/	/	/
	Deep	187	193	169	157	177
Weighted mean depth (m)	Shallow	128	148	/	/	/
	Deep	208	218	203	160	189
Max depth (m)	Shallow	160	161	/	/	/
	Deep	230	243	236	164	201
Depth range (m)	Shallow	61	27	/	/	/
	Deep	44	50	67	7	24
PAR max ($\mu\text{mol m}^{-2} \text{s}^{-1}$)	Shallow	9×10^{-3}	4×10^{-3}	/	/	/
	Deep	1×10^{-5}	5×10^{-5}	3×10^{-5}	1×10^{-4}	4×10^{-5}
PAR min ($\mu\text{mol m}^{-2} \text{s}^{-1}$)	Shallow	1×10^{-4}	6×10^{-4}	/	/	/
	Deep	5×10^{-7}	1×10^{-6}	2×10^{-7}	6×10^{-5}	7×10^{-6}
PAR span (orders of magnitude)	Shallow	2	0.9	/	/	/
	Deep	1.4	1.6	2.2	0.2	0.8

Layers are defined as median backscatter > -68 dB, where shallow layers reside in the upper 150 m and deep layers below.

Aggregations

Maurolicus formed aggregations which varied strongly in vertical extent, size, and apparent behaviour, depending also on the frequency and distance from the observing echosounder (Figure S5). The deeper winter layer (>150 m) usually had low density (mean S_v values < -65 dB; Figure 2), although, on about 50% of the winter days, dense aggregations ($S_v > -63$ dB) formed at depths beyond 125 m (Figures 3 and 4a). In contrast, dense aggregations (mean $S_v > -63$ dB) regularly formed in the shallowest (<100 m) layers during daytime (Figure 4b). In winter, such group formation occurred mainly at PAR levels $>5 \times 10^{-3} \mu\text{mol m}^{-2} \text{s}^{-1}$ (Figure 2). From about mid-April though, the deeper and shallow layers fused and formed tight aggregations at light levels of about $5 \times 10^{-5} \mu\text{mol m}^{-2} \text{s}^{-1}$ (Figure 2).

Bold individuals and individuals moving between main layers

Particularly in February/March and April/May, individuals and small groups of *M. muelleri* were located shallower, sometimes more than 40 m, than the upper-most daytime scattering layer (e.g. Figure 5; more examples in Supplementary Figure S6). The association of these “bold individuals” with the shallow main layer was evident from observations of individuals returning to or ascending from the main layer (Figures 5 and 6, Supplementary Figure S6). Both the main layer and the bold individuals responded upon sudden increases or decreases in surface light by downward or upward swimming, respectively (Supplementary Figure S6). Yet, the bold individuals were exposed to light levels up to ~ 1.5 orders of magnitude higher than the light intensity of the shallowest part of the main layer.

Individuals also switched between the main layers (Figure 6a, Supplementary Figure S7), solitarily or in small groups. The distance between the main scattering layers was on average around 25 m between November and December, around 20 m in January and decreased strongly thereafter (Figure 2). Thus, individuals switching between the main layers crossed on average 0.8 orders of magnitude of ambient light in late December, and about 0.6 orders of magnitude in January with $K_d = 0.0739$ (Figure 2). Individuals swam between layers at vertical velocities between 0.5

and 2.5 cm s^{-1} . Some of the individuals moved in a step-wise pattern (Figure 6).

Encounter with predators

Potential predators of *M. muelleri* appeared as strong echo traces in the echograms. During the daytime, *M. muelleri* often suddenly dived into deeper waters upon encounter with such strong fish echoes (Figure 7). This type of response occurred in the upper scattering layer, in small groups, and in individually swimming fish. Sometimes, the diving led to a cascading effect with vertical relocations manifesting out to a range of more than 50 m from the triggering echo (Figure 7a). Vertical velocities during diving were between 5 and 20 cm s^{-1} over a short time period (usually <1 min). We observed dive reactions at ambient light levels between 10^{-6} and $10^{-1} \mu\text{mol m}^{-2} \text{s}^{-1}$ (Figure 8a). Most dives happened at light levels between 10^{-4} and $10^{-2} \mu\text{mol m}^{-2} \text{s}^{-1}$. Both predator presence and the proportion of dive reactions upon predator encounter increased with increasing light (Figure 8c).

Discussion

We demonstrate that the flexible behaviour of *Maurolicus muelleri* strongly modulates the appearance of acoustic scattering layers. Ten months of recordings provided continuous high-resolution data throughout the water column and resolved novel individual behavioural patterns, reflecting variation in risk taking, and adding to seasonal and short-term population patterns. In addition to individuals swimming within the main scattering layers, we discerned three individual behavioural patterns; as (i) bold individuals that apparently took a higher risk by swimming into more illuminated waters above the main population, (ii), individuals that switched between the main scattering layers, and (iii) individuals that apparently reduced predation risk by swimming away from predators.

Both the environment, other animals and individual state modulate behaviour including vertical distribution. Light appears to be the primary environmental factor modulating the vertical distribution of mesopelagic scattering layers (Kampa and Boden, 1954; Dickson, 1972; Aksnes et al., 2017), although temperature and oxygen may also play a role (Netburn and Koslow, 2015). In addition, fish size and ontogeny, with associated variation in visibility and physiology determine the vertical distributions of

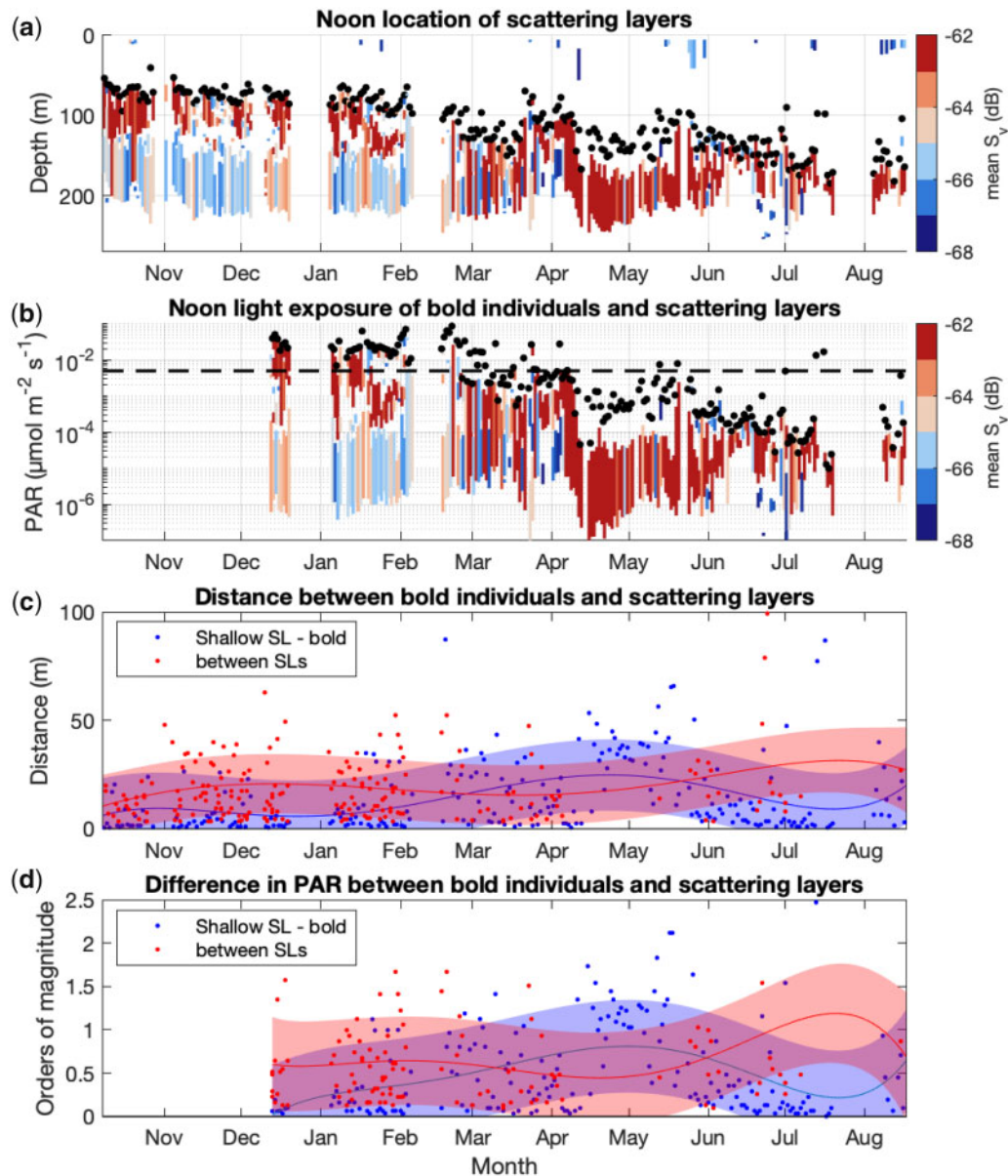


Figure 3. Noon location (a) and light exposure (b) of scattering layers (SL; coloured bars and dots) and bold individuals (black dots). The colours represent the average volume backscatter (S_v) of the respective layer. The vertical distance between bold individuals and the uppermost scattering layer (blue dots) as well as between the scattering layers (red dots) is indicated in metres (c) and orders of magnitude in PAR (d).

pearlsides (Giske *et al.*, 1990; Baliño and Aksnes, 1993; Staby *et al.*, 2013). The ambient light conditions for the main pearlside layers (Figure 3, Table 2) are consistent with previous observations (Rasmussen and Giske, 1994; Staby and Aksnes, 2011; Røstad *et al.*, 2016) and confirm that most pearlsides within a particular scattering layer are exposed to a similar range of light conditions throughout the day.

The fact that the light intensity of the upper and lower edges of the scattering layers differ substantially, supports the concept of a light comfort zone (Røstad *et al.*, 2016) where individual fish avoid both too high and too low illumination (Dupont *et al.*, 2009). Our data thus contrast the traditional “isolume hypothesis” (Clarke and Backus, 1957; Frank and Widder, 2002), where individuals are assumed to be attracted by a specific light

intensity. Our results suggest strong seasonal variation in the pearlside’s light comfort zone as indicated by the thickness of their scattering layers (very narrow in summer). Increased light attenuation is expected to narrow a specific light comfort zone (Røstad *et al.*, 2016) but is unable to account for the variation in thickness seen here. Our observations rather suggest that the light comfort zone of *M. muelleri* is dynamic and emerges from the individual state in addition to size-related differences in vertical distribution (Giske *et al.*, 1990; Baliño and Aksnes, 1993; Staby *et al.*, 2013). Also, bolder fish which explored depths that are out of the comfort zone of most of the population likely add to the variation in comfort zones.

The variation in light comfort zones is supported by our observations of individuals which in a short time crossed light

gradients both within and between layers (individuals moving between layers) as well as appearing outside, and shallower than, the main layers (bold individuals). The data do not allow for assessing if the bold individuals repeatedly and consistently acted “atypically”, thus being specialized individuals (Bolnick *et al.*, 2003; Sih *et al.*, 2015), or if deviating behaviour was state-related

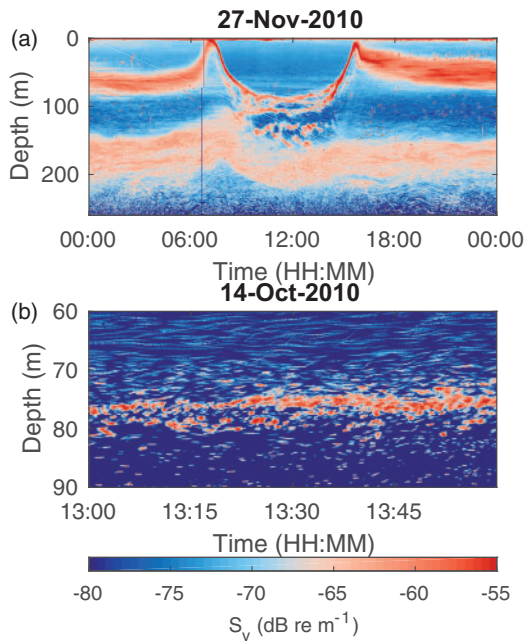


Figure 4. Aggregations formed during daytime by *Maurolicus muelleri* as seen from the 120 kHz (a) and 200 kHz (b) echosounder.

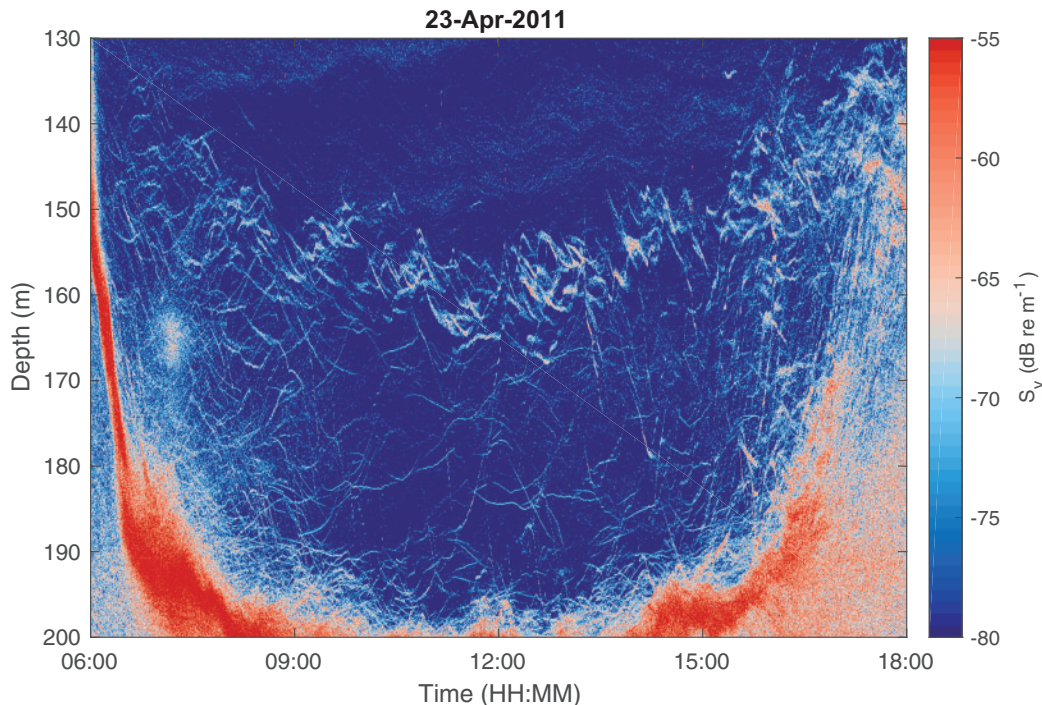


Figure 5. Example of bold individuals, which stayed at shallower depths than the main layers during the day, as observed from the 120 kHz echosounder.

(e.g. hunger) and could occur in any individual (Sih *et al.*, 2015). Nevertheless, in addition to the established importance of light and fish size, the switching between layers reported here likely unveils the impact of some internal motivation. Internal state or individuals more willing to take risks (Sih *et al.*, 2015) may thus lead to deviations from the assumed size-dependent depth distribution. Larger individuals, which are most frequent at depth, may move to a shallower layer consisting of mostly smaller individuals, and vice versa. Future research with high-resolution target sampling could test this hypothesis. Furthermore, net sampling on bold individuals could elucidate if certain groups (age, size, sex, maturity, and stomach fullness) prevailed among these individuals, to provide further indications of reasons for their apparently different risk assessment.

Animals have sophisticated behavioural repertoires to avoid predation and the actual risk of being eaten is affected by the probability to be detected by a predator and the probability of a successful escape (Lima and Dill, 1990). In the pelagic environment, prey may adopt several strategies to mitigate the risk of visual predation. The most apparent anti-predator behaviour of animals in mesopelagic scattering layers is continuously hiding in relatively dark waters, such as in diel vertical migration (Clarke and Backus, 1957; Clark and Levy, 1988). In addition, reports of schooling mesopelagic fish exist (Barham, 1970; Saunders *et al.*, 2013). Recent research has also highlighted social interactions in response to predators in the mesopelagic zone (Benoit-Bird *et al.*, 2017). Daytime schooling of myctophids (Saunders *et al.*, 2013), other mesopelagic fish (Marchal, 1996), and also pearlsides (Gauthier *et al.*, 2014), in the epipelagic zone has been reported. Our close-range, highly resolved data show both flexibility in vertical migration and group dynamics on different time scales. In addition to their vertical migration, the pearlsides formed tight

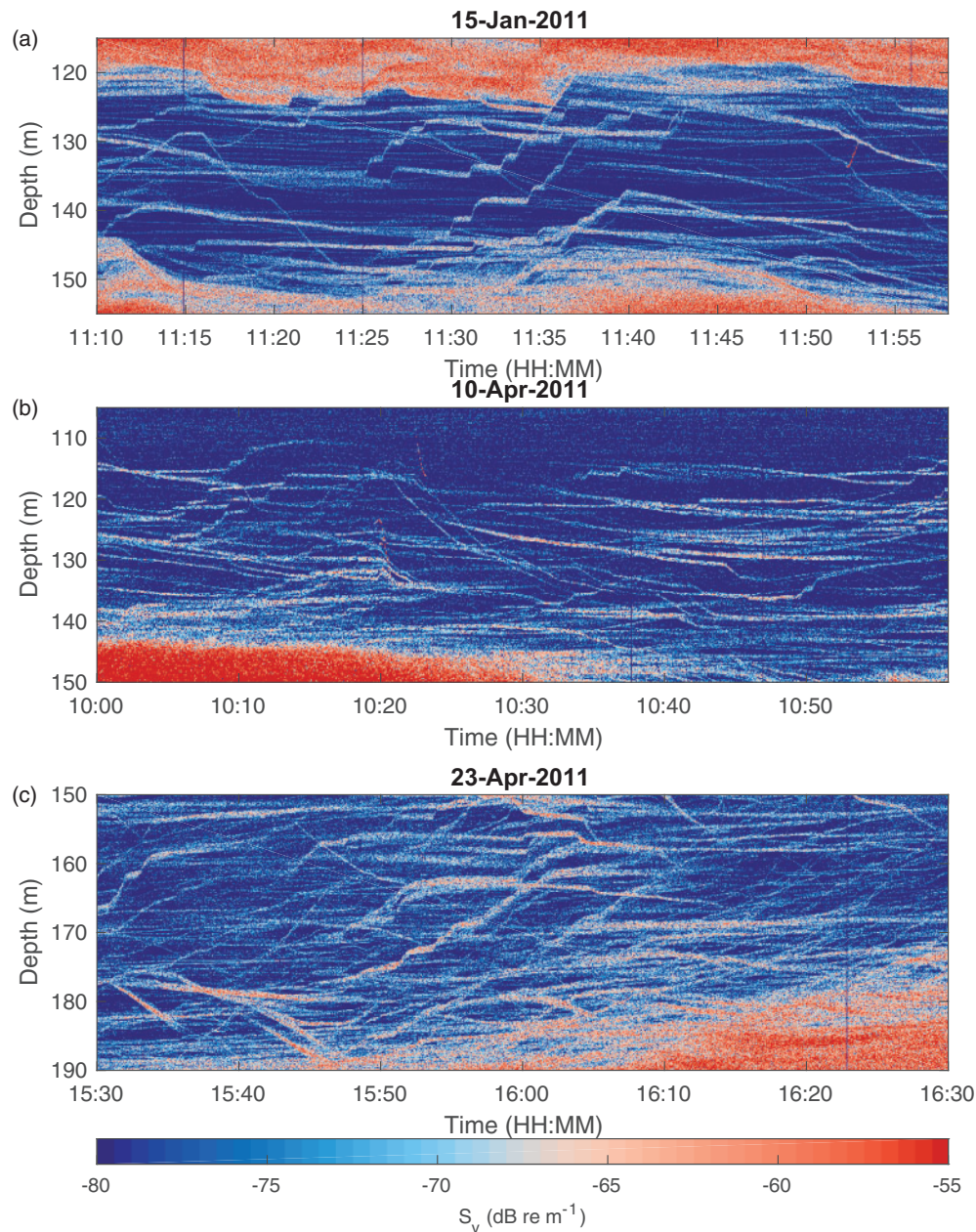


Figure 6. Echo traces of individuals moving between scattering layers and above the upper scattering layer as observed with the 120 kHz echosounder. (a) Relocations between a deep and shallow layer, (b) and (c) bold individuals relocating above the shallowest layer. Some of the fish use a step-wise swimming behaviour during relocation.

groups in the upper scattering layer during daytime. Pearlsides thus appear capable of optimizing their response to a dynamically changing environment using a combination of vertical distribution and social interactions. Probably, the social interactions allow for behaviours that would be sub-optimal for single individuals (Ritz *et al.*, 2011). Social interactions and aggregations may thereby modify the species' realized niche, in this case, their light comfort zone.

While schools may be beneficial under certain (light) conditions, large aggregations are likely more conspicuous than smaller groups (Ritz *et al.*, 2011). Additionally, a main drawback of grouping is intraspecific competition for resources

(Parrish and Edelstein-Keshet, 1999). Optimal group size therefore varies dynamically “as a function of resources, physiology, predominant activity, and limitations of the sensing abilities of the members” (Parrish and Edelstein-Keshet, 1999). The bold individuals regularly formed small groups which occupied depths with light levels up to 1.5 orders of magnitude higher than at the upper edge of “their” layer. They thus seemed to take more risk than the majority of the population, yet also with enhanced chances of reward in their visual search for prey (see below). Bold individuals returned to or ascended from the main layer at different times of the day. This suggests that a decision to leave the main layer could be

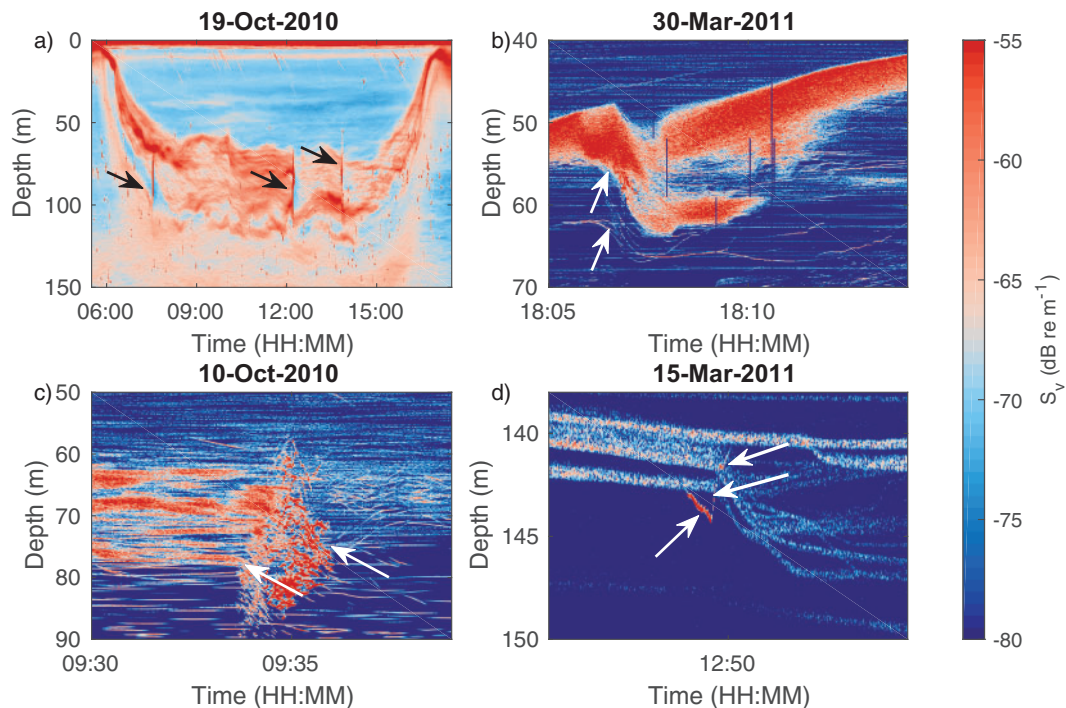


Figure 7. Reactions of *Maurolicus muelleri* interpreted as encounter with predators (highlighted by arrows). (a) Sudden displacements of the scattering layer (by more than 50 m) interpreted as cascading dive responses. (b) *M. muelleri* dive and split into two vertical layers during the dusk ascent, the vertical lines are noise, (c) The scattering layer dives and partly splits at daytime, (d) a potential predator first swims down but then ascends quickly, possibly attacking a group of *M. muelleri* from below. The pearlsides start diving only upon direct encounter. The echograms in (a) and (d) are reproduced from the 120 kHz data, (b) and (c) from the 200 kHz data.

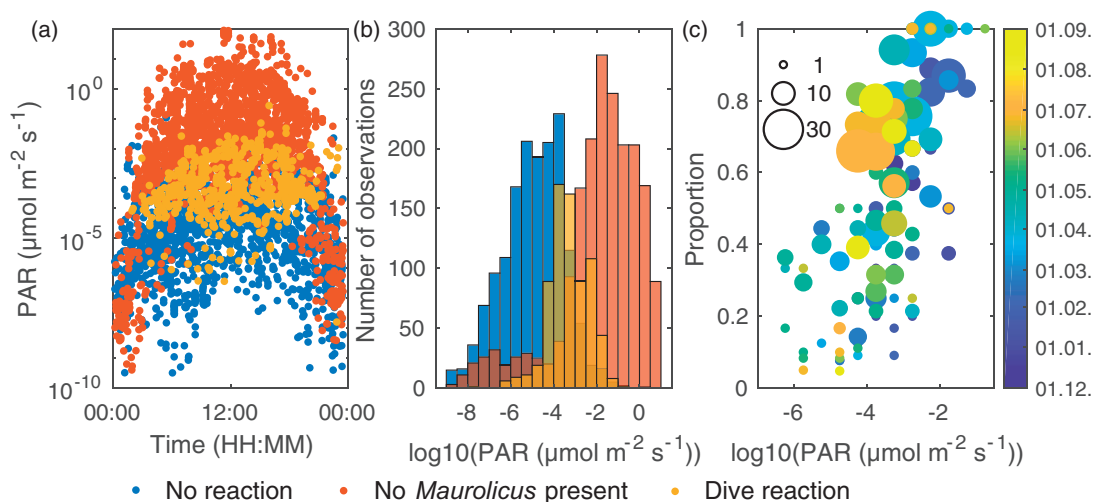


Figure 8. Light intensity at depths where potential predators (strong echo traces on the echogram) were observed as a function of the time of day (a). The histogram (b) shows the corresponding frequency distribution. The colours in (a) and (b) show the type of reaction by *Maurolicus muelleri*. Panel (c) shows the proportion of encounters between potential predators and *M. muelleri* that resulted in a dive reaction. The size of the circles indicates how many dive reactions were observed at the respective light level and day.

state-dependent, as suggested for other mesopelagic species (Dypvik *et al.*, 2012).

Animals constantly have to manage the benefits and risks of what they do, and reasons for observed behaviour may be manifold. One possible and plausible reason for leaving the main layer could be hunger. In winter in Masfjorden, zooplankton biomass

is highest at depths deeper than ~ 70 m (Rosland and Giske, 1997), and some pearlsides feed during the daytime in winter (Bagoien *et al.*, 2001). The light exposure of the bold groups was in the same order of magnitude as that in surface waters at dusk and dawn, and would thus likely be sufficient for visual feeding with the pearlside's twilight-adapted retina

(de Busserolles *et al.*, 2017). Bold behaviour could thus reflect hungry pearlsheds making brief feeding trips to shallower waters and returning to safer depths when satiated. Similarly, behaviour could be related to differential spawning status during spring (Melo and Armstrong, 1991).

Vertical swimming speeds of individuals switching between layers were usually 1–2 cm s⁻¹, which correspond to <1 body length s⁻¹. Animals move at a range of velocities, depending on their requirements for energy conservation, migration, foraging, and predator avoidance (Beamish, 1978; Nathan *et al.*, 2008; Fernö *et al.*, 2011). The values reported here are comparable to those of nocturnal swimming velocities in juvenile pearlsheds (Christiansen *et al.*, 2019) and other mesopelagic fish (Torgersen and Kaartvedt, 2001). The step-wise migration pattern may represent a way of reducing the risk of predation when outside of larger groups, as the fish tilt angle may affect the benefit of counter illumination by their prominent ventral light organs (cf. Christiansen *et al.*, 2019). In contrast, vertical escape reactions were rapid. The pearlsheds reacted to encounter with potential predators, likely larger gadoid fishes, by diving at speeds up to 15–20 cm s⁻¹.

The pearlsheds' escape reactions indicated that the mesopelagic fish sense predators at several metres distance. Fish may detect predators visually (Kelley and Magurran, 2003), by olfactory cues (Dixon *et al.*, 2010), by sensing pressure waves emitted by the predator (Stewart *et al.*, 2014) or by a combination of senses. Escape diving was recorded both among bold individuals (Figures 6b and 7d) and scattering layers and sometimes led to cascading reactions, similar to the “escape waves” described by Herbert-Read *et al.* (2015). Escape reactions only appeared between light levels of 10⁻⁶ and 10⁻¹ μmol m⁻² s⁻¹. This indicates a visual response, with a threshold level of ca. 10⁻⁶ μmol m⁻² s⁻¹. The lack of dive reactions at light levels below this suggests that bioluminescence did not matter for avoidance.

Conclusion

The pearlsheds *Maurolicus muelleri* has a rich repertoire of behaviours and various distribution patterns. Although the fish mainly seem to react upon changes in the environment (especially light, but also predators), we could also clearly observe individuals deviating from the main population behaviour. These individuals actively seeked higher or lower risk areas, potentially due to difference in satiation state and risk aversion, and thus showed some level of decision making (Lima and Dill, 1990). Furthermore, social interactions seem to play an important role in defining the fishes light comfort zone. The variability in behaviour of the single species analysed here can only be a small representation of the true variability found in the open ocean, where mesopelagic scattering layers may consist not of one or two, but more than 100 fish species (Ariza *et al.*, 2016; Wang *et al.*, 2019). Nevertheless, we show that high-resolution and long-term observations can reveal diverse aspects of life in one of the most unexplored regions on our planet and broaden our knowledge about this vast ecosystem.

Supplementary data

Supplementary material is available at the ICES/JMS online version of the manuscript.

Acknowledgements

The field work was funded by King Abdullah University of Science and Technology (KAUST). D.L.A. and S.K. were supported by the EU-project SUMMER (Grant agreement number: 817806) during preparation of the manuscript. We would like to thank Rita Amundsen, Ingrid Solberg, Eivind Dypvik, Perdana Karim Prihartato, and the crew of RV Trygve Braarud for their assistance during the field work. We would like to thank two anonymous reviewers for their very helpful suggestions and Josefin Titelman for providing valuable comments during manuscript revision.

Author contributions

This study was conceptualized by S.K. S.C. analysed and visualized the data. T.A.K., A.R. and D.L.A. collected the data. S.C. and S.K. wrote the first version of the manuscript. All authors contributed to the further writing of the article.

Data availability

The echosounder data underlying this article are available at the Norwegian Marine Data Centre and can be accessed with <http://metadata.nmdc.no/metadata-api/landingpage/73073a8b13dad04344dc9ecfa4280453>. The light data will be shared on reasonable request to the corresponding author.

References

- Aksnes, D. L., Aure, J., Johansen, P.-O., Johnsen, G. H., and Vea Salvanes, A. G. 2019. Multi-decadal warming of Atlantic water and associated decline of dissolved oxygen in a deep fjord. *Estuarine, Coastal and Shelf Science*, 228: 106392–106398.
- Aksnes, D. L., Røstad, A., Kaartvedt, S., Martinez, U., Duarte, C. M., and Irigoien, X. 2017. Light penetration structures the deep acoustic scattering layers in the global ocean. *Science Advances*, 3: e1602468–5.
- Allen, P. M., and McGlade, J. M. 1987. Evolutionary drive: the effect of microscopic diversity, error making, and noise. *Foundations of Physics*, 17: 723–738.
- Allgeier, J. E., Cline, T. J., Walsworth, T. E., Wathen, G., Layman, C. A., and Schindler, D. E. 2020. Individual behavior drives ecosystem function and the impacts of harvest. *Science Advances*, 6: eaax8329.1–9.
- Ariza, A., Landeira, J. M., Escáñez, A., Wienerroither, R., de Soto, N. A., Røstad, A., Kaartvedt, S., *et al.* 2016. Vertical distribution, composition and migratory patterns of acoustic scattering layers in the Canary Islands. *Journal of Marine Systems*, 157: 82–91.
- Bagøien, E., Kaartvedt, S., Aksnes, D. L., and Eiane, K. 2001. Vertical distribution and mortality of overwintering *Calanus*. *Limnology and Oceanography*, 46: 1494–1510.
- Baliño, B. M., and Aksnes, D. L. 1993. Winter distribution and migration of the sound scattering layers, zooplankton and micronekton in Masfjorden, western Norway. *Marine Ecology Progress Series*, 95: 35–50.
- Balk. 2019. Sonar4 and Sonar5-Pro post processing systems, Operator manual version 606.16, 489 p. CageEye A/S.
- Barham, E. G. 1957. The ecology of sonic scattering layers in the Monterey bay area. 196 pp.
- Barham, E. G. 1966. Deep scattering layer migration and composition: observations from a diving saucer. *Science*, 151: 1399–1403.
- Barham, E. G. 1970. Deep-sea fishes. Lethargy and vertical orientation. *In Proceedings of International Symposium on Biological Sound Scattering in the Ocean*, pp. 100–116. Ed. by G. B. Farquhar. U.S. Government Printing Office, Washington, DC.

- Beamish, F. W. H. 1978. Swimming capacity. *In* Fish Physiology, pp. 101–187. Ed. by W. S. Hoar and D. J. Randall. Academic Press, Inc. 87 pp.
- Belcher, A., Saunders, R. A., and Tarling, G. A. 2019. Respiration rates and active carbon flux of mesopelagic fishes (Family Myctophidae) in the Scotia Sea, Southern Ocean. *Marine Ecology Progress Series*, 610: 149–162.
- Benoit-Bird, K. J., Moline, M. A., and Southall, B. L. 2017. Prey in oceanic sound scattering layers organize to get a little help from their friends. *Limnology and Oceanography*, 62: 2788–2798.
- Béghale, N., Cotté, C., Ryan, T. E., Gauthier, O., Roudaut, G., Brehmer, P., Josse, E., *et al.* 2016. Acoustic micronektonic distribution is structured by macroscale oceanographic processes across 20–50°S latitudes in the South-Western Indian Ocean. *Deep-Sea Research Part I*, 110: 20–32.
- Bolnick, D. I., Svanbäck, R., Fordyce, J. A., Yang, L. H., Davis, J. M., Hulseley, C. D., and Forister, M. L. 2003. The ecology of individuals: incidence and implications of individual specialization. *The American Naturalist*, 161: 1–28.
- Boswell, K. M., D'Elia, M., Johnston, M. W., Mohan, J. A., Warren, J. D., Wells, R. J. D., and Sutton, T. T. 2020. Oceanographic structure and light levels drive patterns of sound scattering layers in a low-latitude oceanic system. *Frontiers in Marine Science*, 7: 1–15.
- Christiansen, S., Titelman, J., and Kaartvedt, S. 2019. Nighttime swimming behavior of a mesopelagic fish. *Frontiers in Marine Science*, 6: 1–12.
- Clark, C. W., and Levy, D. A. 1988. Diel vertical migrations by juvenile sockeye salmon and the antipredation window. *The American Naturalist*, 131: 271–290.
- Clarke, G. L., and Backus, R. H. 1957. Measurements of light penetration in relation to vertical migration and records of luminescence of deep-sea animals. *Deep Sea Research (1953)*, 4: 1–14.
- Davison, P. C., Koslow, J. A., and Kloser, R. J. 2015. Acoustic biomass estimation of mesopelagic fish: backscattering from individuals, populations, and communities. *ICES Journal of Marine Science*, 72: 1413–1424.
- de Busserolles, F., Cortesi, F., Helvik, J. V., Davies, W. I. L., Templin, R. M., Sullivan, R. K. P., Michell, C. T., *et al.* 2017. Pushing the limits of photoreception in twilight conditions: the rod-like cone retina of the deep-sea pearlshades. *Science Advances*, 3: eaao4709–eaao4712.
- Dickson, R. R. 1972. On the relationship between ocean transparency and the depth of sonic scattering layers in the North Atlantic. *ICES Journal of Marine Science*, 34: 416–422.
- Dietz, R. S. 1948. Deep scattering layer in the Pacific and Antarctic Oceans. *Journal of Marine Research*, 7: 430–442.
- Dixon, D. L., Munday, P. L., and Jones, G. P. 2010. Ocean acidification disrupts the innate ability of fish to detect predator olfactory cues. *Ecology Letters*, 13: 68–75.
- Dupont, N., Klevjer, T. A., Kaartvedt, S., and Aksnes, D. L. 2009. Diel vertical migration of the deep-water jellyfish *Periphylla periphylla* simulated as individual responses to absolute light intensity. *Limnology and Oceanography*, 54: 1765–1775.
- Duvall, G. E., and Christensen, R. J. 1946. Stratification of sound scatterers in the ocean. *The Journal of the Acoustical Society of America*, 18: 254–254.
- Dypvik, E., Røstad, A., and Kaartvedt, S. 2012. Seasonal variations in vertical migration of glacier lanternfish, *Benthosema glaciale*. *Marine Biology*, 159: 1673–1683.
- Engås, A., Skeide, R., and West, C. W. 1997. The 'MultiSampler': a system for remotely opening and closing multiple codends on a sampling trawl. *Fisheries Research*, 29: 295–298.
- Escobar-Flores, P. C. 2019. Acoustic assessment of the micronekton community on the Chatham Rise, New Zealand, using a semi-automated approach. *Frontiers in Marine Science*, 6: 1–22.
- Eyring, C. F., Christensen, R. J., and Raitt, R. W. 1948. Reverberation in the Sea. *The Journal of the Acoustical Society of America*, 20: 462–475.
- Fernö, A., Jørgensen, T., Løkkeborg, S., and Winger, P. D. 2011. Variable swimming speeds in individual Atlantic cod (*Gadus morhua* L.) determined by high-resolution acoustic tracking. *Marine Biology Research*, 7: 310–313.
- Foote, K. G., Knudsen, H. P., Vestnes, G., MacLennan, D., and Simmonds, J. 1987. Calibration of acoustic instruments for fish density estimation. 144. 69 pp.
- Frank, T., and Widder, E. 2002. Effects of a decrease in downwelling irradiance on the daytime vertical distribution patterns of zooplankton and micronekton. *Marine Biology*, 140: 1181–1193.
- Gauthier, S., Oeffner, J., and O'Driscoll, R. L. 2014. Species composition and acoustic signatures of mesopelagic organisms in a subtropical convergence zone, the New Zealand Chatham Rise. *Marine Ecology Progress Series*, 503: 23–40.
- Giske, J., Aksnes, D. L., Baliño, B. M., Kaartvedt, S., Lie, U., Nordeide, J. T., Salvanes, A. G. V., *et al.* 1990. Vertical distribution and trophic interactions of zooplankton and fish in Masfjorden, Norway. *Sarsia*, 75: 65–81.
- Grimaldo, E., Grimsmo, L., Alvarez, P., Herrmann, B., Møen Tveit, G., Tiller, R., Slizyte, R., *et al.* 2020. Investigating the potential for a commercial fishery in the Northeast Atlantic utilizing mesopelagic species. *ICES Journal of Marine Science*, 9: 76–16.
- Herbert-Read, J. E., Buhl, J., Hu, F., Ward, A. J. W., and Sumpter, D. J. T. 2015. Initiation and spread of escape waves within animal groups. *Royal Society Open Science*, 2: 140355–140311.
- Hudson, J. M., Steinberg, D. K., Sutton, T. T., Graves, J. E., and Latour, R. J. 2014. Myctophid feeding ecology and carbon transport along the northern Mid-Atlantic Ridge. *Deep-Sea Research Part I*, 93: 104–116.
- Kampa, E. M., and Boden, B. P. 1954. Submarine illumination and the twilight movements of a sonic scattering layer. *Nature*, 174: 869–871.
- Kelley, J. L., and Magurran, A. E. 2003. Learned predator recognition and antipredator responses in fishes. *Fish and Fisheries*, 4: 216–226.
- Lima, S. L., and Dill, L. M. 1990. Behavioral decisions made under the risk of predation: a review and prospectus. *Canadian Journal of Zoology-Revue Canadienne De Zoologie*, 68: 619–640.
- MacLennan, D., Fernandes, P. G., and Dalen, J. 2002. A consistent approach to definitions and symbols in fisheries acoustics. *ICES Journal of Marine Science*, 59: 365–369.
- Marchal, E. 1996. Acoustic evidence for unusual diel behaviour of a mesopelagic fish (*Vinciguerria nimbaria*) exploited by tuna. *ICES Journal of Marine Science*, 53: 443–447.
- Melo, Y. C., and Armstrong, M. J. 1991. Batch spawning behaviour in lightfish *Maurollicus muelleri*. *South African Journal of Marine Science*, 10: 125–130.
- Nathan, R., Getz, W. M., Revilla, E., Holyoak, M., Kadmon, R., Saltz, D., and Smouse, P. E. 2008. A movement ecology paradigm for unifying organismal movement Research. *Proceedings of the National Academy of Sciences of the United States of America*, 105: 19052–19059.
- Netburn, A. N., and Koslow, J. A. 2015. Dissolved oxygen as a constraint on daytime deep scattering layer depth in the southern California current ecosystem. *Deep-Sea Research Part I*, 104: 149–158.
- Parrish, J. K., and Edelman-Keshet, L. 1999. Complexity, pattern, and evolutionary trade-offs in animal aggregation. *Science*, 284: 99–101.
- Pearcy, W. G., Krygier, E. E., Mesecar, R., and Ramsey, F. 1977. Vertical distribution and migration of oceanic micronekton off Oregon. *Deep-Sea Research*, 24: 223–245.

- Prellezo, R. 2019. Exploring the economic viability of a mesopelagic fishery in the Bay of Biscay. *ICES Journal of Marine Science*, 76: 771–779.
- Prihartato, P. K., Aksnes, D. L., and Kaartvedt, S. 2015. Seasonal patterns in the nocturnal distribution and behavior of the mesopelagic fish *Maurolicus muelleri* at high latitudes. *Marine Ecology Progress Series*, 521: 189–200.
- Proud, R., Cox, M. J., and Brierley, A. S. 2017. Biogeography of the global ocean's mesopelagic zone. *CURBIO*, 27: 113–119.
- Proud, R., Handegard, N. O., Kloser, R. J., Cox, M. J., and Brierley, A. S. 2019. From siphonophores to deep scattering layers: uncertainty ranges for the estimation of global mesopelagic fish biomass. *ICES Journal of Marine Science*, 76: 718–733.
- Rasmussen, O. I., and Giske, J. 1994. Life-history parameters and vertical distribution of *Maurolicus muelleri* in Masfjorden in summer. *Marine Biology*, 120: 649–664.
- Rees, D. J., Poulsen, J. Y., Sutton, T. T., Costa, P. A. S., and Landaeta, M. F. 2020. Global phylogeography suggests extensive eucosmopolitanism in Mesopelagic Fishes (*Maurolicus*: sternoptychidae). *Scientific Reports*, 10: 20544. 1–12.
- Ritz, D. A., Hobday, A. J., Montgomery, J. C., and Ward, A. J. W. 2011. Social aggregation in the pelagic zone with special reference to fish and invertebrates. In *Advances in Marine Biology*, p 161–227. Ed. by M. Lesser, Academic Press
- Rosland, R., and Giske, J. 1997. A dynamic model for the life history of *Maurolicus muelleri*, a pelagic planktivorous fish. *Fisheries Oceanography*, 6: 19–34.
- Rudstam, L. G., Knudsen, F. R., Balk, H., Gal, G., Boscarino, B. T., and Axenrot, T. 2008. Acoustic characterization of *Mysis relicta* at multiple frequencies. *Canadian Journal of Fisheries and Aquatic Sciences*, 65: 2769–2779.
- Røstad, A., Kaartvedt, S., and Aksnes, D. L. 2016. Light comfort zones of mesopelagic acoustic scattering layers in two contrasting optical environments. *Deep-Sea Research Part I*, 113: 1–6.
- Saunders, R. A., Fielding, S., Thorpe, S. E., and Tarling, G. A. 2013. School characteristics of mesopelagic fish at South Georgia. *Deep-Sea Research Part I*, 81: 62–77.
- Sih, A., Mathot, K. J., Moirón, M., Montiglio, P.-O., Wolf, M., and Dingemanse, N. J. 2015. Animal personality and state-behaviour feedbacks: a review and guide for empiricists. *Trends in Ecology & Evolution*, 30: 50–60.
- Staby, A., and Aksnes, D. L. 2011. Follow the light—diurnal and seasonal variations in vertical distribution of the mesopelagic fish *Maurolicus muelleri*. *Marine Ecology Progress Series*, 422: 265–273.
- Staby, A., Røstad, A., and Kaartvedt, S. 2011. Long-term acoustical observations of the mesopelagic fish *Maurolicus muelleri* reveal novel and varied vertical migration patterns. *Marine Ecology Progress Series*, 441: 241–255.
- Staby, A., Srisomwong, J., and Rosland, R. 2013. Variation in DVM behaviour of juvenile and adult pearlside (*Maurolicus muelleri*) linked to feeding strategies and related predation risk. *Fisheries Oceanography*, 22: 90–101.
- Stewart, W. J., Nair, A., Jiang, H., and McHenry, M. J. 2014. Prey fish escape by sensing the bow wave of a predator. *The Journal of Experimental Biology*, 217: 4328–4336.
- Torgersen, T., and Kaartvedt, S. 2001. In situ swimming behaviour of individual mesopelagic fish studied by split-beam echo target tracking. *ICES Journal of Marine Science*, 58: 346–354.
- Urmy, S. S., and Horne, J. K. 2016. Multi-scale responses of scattering layers to environmental variability in Monterey Bay. *California. Deep-Sea Research Part I*, 113: 22–32.
- Wang, X., Zhang, J., Zhao, X., Chen, Z., Ying, Y., Li, Z., Xu, D., *et al.* 2019. Vertical distribution and diel migration of mesopelagic fishes on the northern slope of the South China Sea. *Deep-Sea Research Part II*, 167: 128–141.
- Welsh, J. H., and Chace, F. A. Jr, 1937. The diurnal migration of deep-water animals. *The Biological Bulletin*, LXXIII: 185–196.

Handling editor: Roland Proud